JETP Letters, Vol. 81, No. 11, 2005, pp. 587–589. Translated from Pis'ma v Zhurnal Éksperimental'noĭ i Teoreticheskoĭ Fiziki, Vol. 81, No. 11, 2005, pp. 721–723.

Two-Band Conductivity of ZrO_2 Synthesized by Molecular Beam Epitaxy

D. V. Gritsenko[1], S. S. Shaĭmeev[1], M. A. Lamin[1], O. P. Pchelyakov[1], V. A. Gritsenko[1], and V. G. Lifshits[2]

[1] *Institute of Semiconductor Physics, Siberian Division, Russian Academy of Sciences, Novosibirsk, 630090 Russia*
e-mail: grits@isp.nsc.ru
[2] *Institute for Automation and Control Processes, Far East Division, Russian Academy of Sciences, Vladivostok, 690041 Russia*
Received May 5, 2005

Using experiments on the injection of minority carriers from *n*- and *p*-type silicon, the contribution of electrons and holes to the conductivity of ZrO_2 in the Si/ZrO_2/Al structure is determined. It is found that electrons and holes make a contribution to the conductivity of ZrO_2, so that ZrO_2 exhibits two-band conductivity. © *2005 Pleiades Publishing, Inc.*

PACS numbers: 77.22.Jp, 77.55.+f, 77.84.Bw

Scaling silicon metal–insulator–semiconductor (MIS) devices is accompanied by a decrease in the channel length and in the thickness of the gate dielectric. Thermal silicon dioxide has been used as a gate dielectric for 40 years. A decrease in the SiO_2 thickness to 10–15 Å is accompanied by an unacceptably high leakage current. The main approach to decreasing the leakage current through the gate dielectric consists in the replacement of silicon dioxide by so-called alternative dielectrics (dielectrics with a high dielectric constant, i.e., high-k dielectrics). The use of alternative dielectrics allows the physical dielectric thickness to be increased and, in this way, the tunnel current to be suppressed [1, 2]. Zirconium dioxide is one of the most promising alternative dielectrics. ZrO_2 has a high dielectric constant ($\varepsilon = 25$), a wide band gap E_g = 5.5 eV, high barriers at the Si/ZrO_2 interface, and high thermodynamic stability of the interface with silicon [3]. In addition, the difference in the lattice constants of Si and ZrO_2 does not exceed 2.1% [4]. The latter circumstance opens the possibility of synthesizing ZrO_2 on Si by molecular beam epitaxy.

In the general case, the contribution to the conductivity of a dielectric is made by electrons and holes [5–7]. The detection of the sign of charge carriers in semiconductors is carried out using either the Hall effect or the thermal emf. In dielectrics, these methods are inapplicable because of the negligibly small concentration of mobile carriers. The goal of this work is to determine the contribution of electrons and holes to the conductivity of dielectric ZrO_2 films synthesized by molecular beam epitaxy in a Si/ZrO_2/Al MIS structure.

We studied Si/ZrO_2/Al structures with *n*- and *p*-type silicon(100) with a resistivity of ≈10 Ω cm. The Si/ZrO_2 structures were obtained in an ultrahigh-vacuum setup Katun'-V by molecular beam epitaxy. High-temperature thermal heating was performed in the setup with the aim of obtaining an atomically clean Si surface. To obtain a ZrO_2 vapor, an electron-beam evaporator was used with the electron beam current I = 250 mA, the voltage U = 6 kV, and magnetic sweep of the electron beam. The target temperature reached 2800–3200°C. The target was single-crystal ZrO_2.

Perfect single-crystal ZrO_2 films (according to electron diffraction data) were obtained on the atomically clean Si surface at substrate temperatures from 400 to 800°C. According to ellipsometric measurements, the ZrO_2 film thickness was in the range 110–300 Å. The measurements of current–voltage and capacity–voltage (100-kHz frequency) characteristics were performed at room temperature. Illumination was performed using a tungsten lamp.

The current–voltage characteristics of the *p*-Si/ZrO_2/Al structure are presented in Fig. 1. The characteristics were obtained at two polarities of the voltage across the metal: in the enhancement mode (a negative potential at Al) and in the depletion mode (a positive potential at Al). In the depletion mode with a positive potential at Al, the saturation of the current is observed in the dark and the current relatively weakly depends on the voltage. The current increases upon switching illumination. The saturation of the current in the depletion mode is related to the injection of minority charge carriers from silicon into the dielectric. In the case of a negative potential at the metal in the enhancement mode, the current increases exponentially with increasing potential. Illumination does not affect the current.

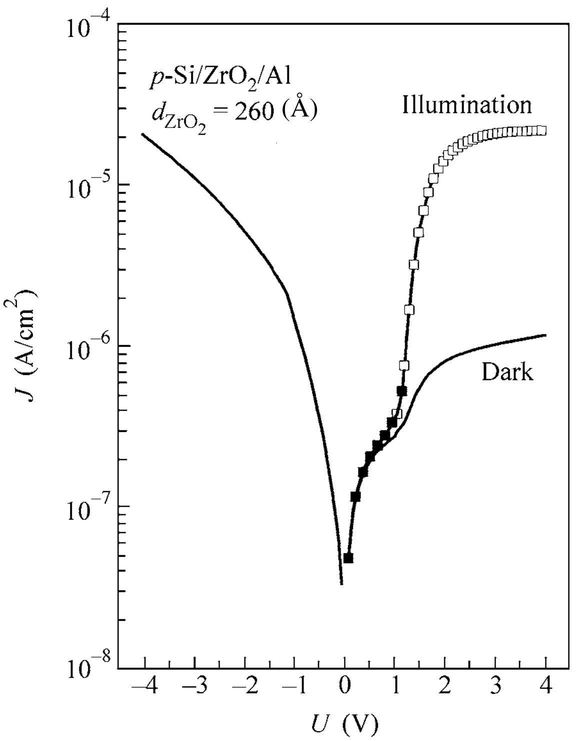

Fig. 1. Current–voltage characteristics of the p-Si/ZrO_2/Al structure obtained (solid lines) in the depletion and enhancement modes and (points) in the depletion mode with illumination.

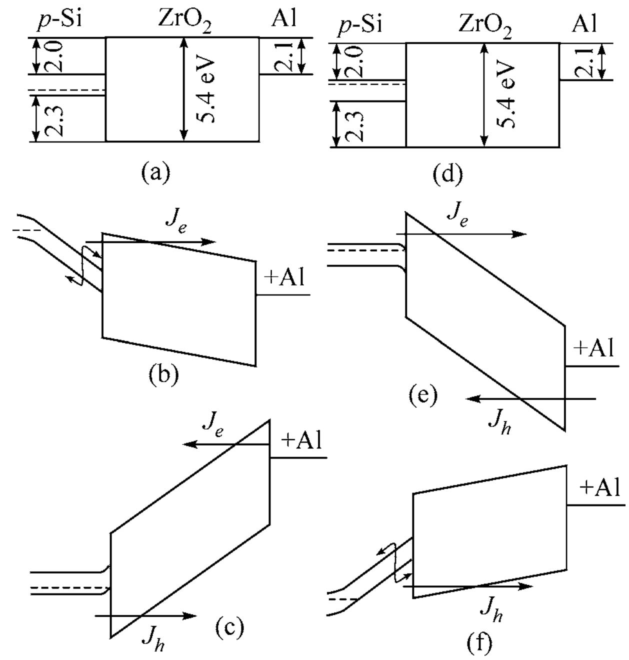

Fig. 2. Energy diagrams of [(a), (b), and (c)] p-Si/ZrO_2/Al and [(d), (e), and (f)] n-Si/ZrO_2/Al structures [(a) and (d)] with no applied voltage, [(b) and (e)] in the depletion mode, and [(c) and (f)] in the enhancement mode.

In this case, virtually all of the applied voltage drops across the dielectric.

The energy diagram of the Si/ZrO_2/Al structure according to the data of photoemission measurements [8] is presented for p- and n-type silicon in Figs. 2a–2f. Figures 2a and 2d show the energy diagram in the flat-band mode without an applied voltage. The ZrO_2 band-gap width is 5.4 eV, and the barrier for electrons at the Si/ZrO_2 interface is 2.0 eV. The energy diagrams of the p-Si/ZrO_2/Al and n-Si/ZrO_2/Al structures are presented in Fig. 2 for a positive potential on the metal (Figs. 2b, 2e) and for a negative potential on the metal (Figs. 2c, 2f).

In the depletion mode in the p-Si/ZrO_2/Al structure, the applied voltage is divided between the dielectric and the nonequilibrium depletion layer (Fig. 2b). This circumstance is caused by the fact that the injection current of minority carriers (electrons) is comparable with their generation rate in silicon. Illumination leads to an increase in the generation rate of minority carriers, to narrowing of the thickness of the depleted layer, to a decrease in the voltage drop across the depletion layer, to an increase in the voltage drop across the dielectric, and, hence, to an increase in the dielectric conductivity. Thus, the behavior of the current–voltage characteristics in the depletion mode indicate that the injection of electrons from silicon makes the main contribution to the ZrO_2 conductivity at a positive potential at aluminum. The flux of holes from the dielectric to silicon is negligibly small as compared to the opposite flux of electrons from silicon to the dielectric. In the case of a negative potential at the metal in the enhancement mode (Fig. 2c), the entire applied voltage drops across the dielectric. It is natural to suggest that the conductivity of the dielectric in this case is also due to electrons injected from aluminum, because the barriers for electrons at the Si/ZrO_2 and Al/ZrO_2 interfaces are close in height (Figs. 2a, 2d).

A similar behavior of the current–voltage characteristics is observed in the n-Si/ZrO_2/Al structure (Fig. 3). In the case of a positive potential at the metal in the enhancement mode, the entire applied voltage drops across the dielectric (Fig. 2e). It is natural to suggest that charge transfer in the dielectric in this case, as well as in the p-Si/ZrO_2/Al structure, is due to electrons injected from silicon (Fig. 2e). In the depletion mode with a negative potential at the metal, the saturation of the current–voltage characteristics is observed (Fig. 3). Illumination leads to an increase in the current level. This means that the nonequilibrium depletion layer is developed by virtue of the injection of holes from silicon into the dielectric (Fig. 2f). Thus, the current to n-Si at the Si/ZrO_2 interface is transferred by holes injected from silicon into the dielectric.

It is natural to suggest that charge transfer in the dielectric in the p-Si/ZrO_2/Al structure at a negative

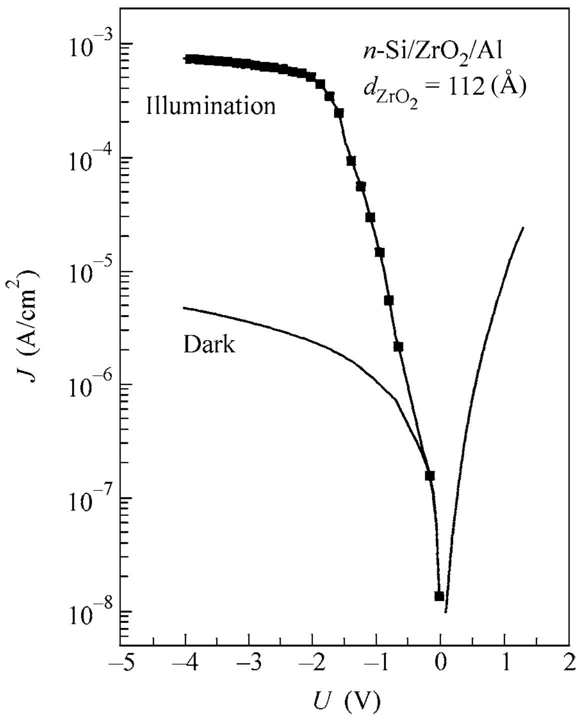

Fig. 3. Same as in Fig. 1, but for the n-Si/ZrO_2/Al structure.

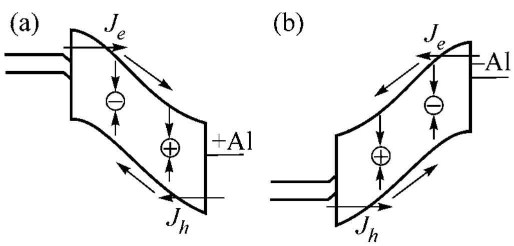

Fig. 4. Schematic diagram of current passage in the Si/ZrO_2/Al structure for (a) positive and (b) negative potentials on the metal. It is assumed that the generation rate of minority carriers in the depletion mode exceeds the rate of their injection into the dielectric.

potential at the metal is also performed by holes injected from silicon (Fig. 2c). In the general case, electrons are injected into the dielectric from a negatively biased electrode and holes are injected into the dielectric from a positively biased electrode. The experiment indicates that ZrO_2 has traps [9, 10]. A two-band model of electron and hole current passage in the Si/ZrO_2/Al structure is presented in Fig. 4 for two polarities of the potential at the metal. According to this model, ZrO_2 contains electron and hole traps, which serve as recombination centers. Consider current passage in more detail for positive polarity of the potential at the metal (Fig. 4a). Electrons are injected from silicon into ZrO_2 and are captured in the traps. Some of electrons are ionized from the traps by the Frenkel mechanism or by the multiphonon mechanism [7, 10]. Next, conduction-band electrons recombine with holes captured in the traps in the vicinity of the anode (metal). Holes from the positively biased metal are injected into the valence band of the dielectric, are captured in the traps, and recombine with free electrons. Some of hole traps are ionized, and the free holes move toward the silicon and recombine with localized electrons. The above model explains the development of a nonequilibrium depletion layer in n-type and p-type silicon due to the injection of minority carriers into the dielectric. A similar pattern is observed for a negative potential at the metal (Fig. 4). The model suggested above is similar to the model of current passage in silicon nitride [6, 7, 11].

This work was supported by the Siberian Division of the Russian Academy of Sciences, integration project no. 116.

REFERENCES

1. A. I. Kingon, J.-P. Maria, and S. K. Streiffor, Nature **406**, 1032 (2000).
2. G. D. Wilk, R. M. Wallace, and J. M. Anthony, J. Appl. Phys. **89**, 5243 (2001).
3. M. Gutowski, J. E. Jaffe, C. L. Liu, *et al.*, Appl. Phys. Lett. **80**, 1897 (2002).
4. Y.-Z. Hu and S.-P. Tau, J. Vac. Sci. Technol. B **19**, 1706 (2001).
5. V. A. Gritsenko, E. E. Meerson, and Yu. N. Morokov, Phys. Rev. B **57**, R2081 (1998).
6. K. A. Nasyrov, Yu. N. Novikov, V. A. Gritsenko, *et al.*, Pis'ma Zh. Éksp. Teor. Fiz. **77**, 455 (2003) [JETP Lett. **77**, 385 (2003)].
7. K. A. Nasyrov, V. A. Gritsenko, Yu. N. Novikov, *et al.*, J. Appl. Phys. **96**, 4293 (2004).
8. V. V. Afanas'ev, M. Houssa, and A. Stesmans, J. Appl. Phys. **91**, 3079 (2002).
9. M. Houssa, M. Tuominen, M. Naili, *et al.*, J. Appl. Phys. **87**, 8615 (2000).
10. S. Ramanathan, C.-M. Park, and P.-C. Mcintyre, J. Appl. Phys. **91**, 4521 (2002).
11. A. S. Ginovker, V. A. Gritsenko, and S. P. Sinitsa, Phys. Status Solidi B **26**, 489 (1974).

Translated by A. Bagatur'yants